J. F. BORGES DA SILVA
Doutor Engenheiro I. S. T.
Prof. Extraordinário do I. S. T.

THE ELECTROSTATIC FIELD PROBLEM OF STRANDED AND BUNDLE CONDUCTORS SOLVED BY THE MULTIPOLE METHOD

Electricidade
N.º 142 — MARÇO-ABRIL 1979

CDU 621.319.7:621.3.015.532
Electric Field
Line Conductors

J. F. BORGES DA SILVA
Doutor Engenheiro I. S. T.
Prof. Extraordinário do I. S. T.

The electrostatic field problem of stranded and bundle conductors solved by the multipole method (*)

ABSTRACT

A general method for handling two-dimensional potential problems involving cylindrical boundaries is presented. An application is made to conductor configurations having n-fold symmetry around an axis, with the main purpose of studying electric field properties in the vicinity of bundle and stranded conductors, such as are commonly used in power transmission line technique. Numerical results obtained for stranded conductors are subjected to accuracy tests and compared with results found in the literature, obtained by different but equally accurate methods. Based on the potential function representation afforded by this method, several properties of stranded conductors, of importance to power transmission line engineering, are investigated and the corresponding numerical results presented in tabular form and as a set of numerical interpolation formulas, facilitating their use in digital computer programs.

RESUMO

Apresenta-se um método geral para o tratamento de problemas relativos à função potencial a duas dimensões, satisfazendo condições fronteira sobre superfícies cilíndricas circulares. Faz-se a sua aplicação ao caso particular de sistemas de condutores que apresentam simetria de ordem-n em torno de um eixo, tendo como objectivo principal o estudo do campo eléctrico na vizinhança da superfície de condutores geminados e entrançados, tal como são usados na técnica das linhas de transmissão de energia. Os resultados numéricos obtidos para condutores entrançados são criticados sob o ponto de vista da precisão que é possível obter, e são comparados com resultados publicados, obtidos por métodos diferentes mas de nível de precisão comparável. Com base na representação da função potencial proporcionada por este método, investigam-se algumas propriedades dos condutores entrançados, importantes para a engenharia das linhas de transmissão de energia e os correspondentes resultados numéricos são apresentados sob a forma de tabelas e também sob a forma de um conjunto de fórmulas numéricas de interpolação, destinadas a facilitar o seu uso em programas de cálculo digital.

1 — INTRODUCTION

In the design of high voltage overhead power transmission lines, knowledge of maximum field intensities occuring at the surface of conductors is required in order to predict the inception of corona discharge and allow estimates to be made of undesirable effects of corona, such as, power loss, radio interference and audible noise.

The starting point for any investigation of these problems consists in obtaining a solution of the potential problem posed by the conducting boundaries involved, sufficiently accurate in their immediate vicinity to allow reliable information regarding surface voltage gradients to be obtained.

As is well known, the requirements of ehv and uhv applications have led to the universal use of bundle conductors (fig. 1), for the phase conductors [1], moreover whether single or as members of a bundle, individual conductors are manufactured as stranded cables (fig. 2), presenting a nearly cylindrical, but non-smooth surface, that must be taken into account in maximum field intensity calculations.

Fortunately, both the bundle and the stranded conductor configurations are geometrically quite similar. Their transversal cross-sections consisting in a set of circular boundaries, having their centers uniformly distributed around a circle so that n-fold symmetry around a central axis results.

The method developed in the present paper is applicable without modification to both problems, the only difference being the number of terms in a series de-

(*) Publicação do Laboratório de Medidas Eléctricas do I.S.T. integrada na actividade da Linha-1 do Centro de Electrotecnia das Universidades de Lisboa, subsidiado pelo I.N.I.C.

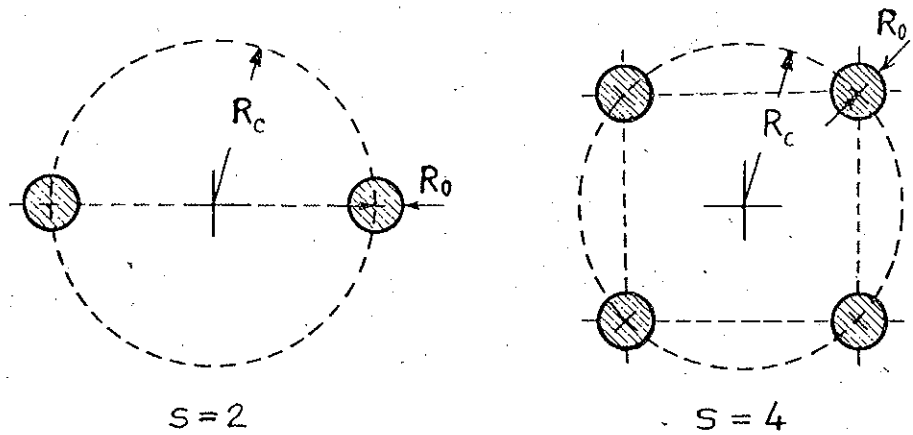

Fig. 1 — *Regular bundle conductors.*

velopment that have to be considered in order to achieve a given accuracy. This number is a function of the subconductor radius to interconductor distance ratio, growing with the latter. The stranded conductor problem having the larger ratio of the two, requires,

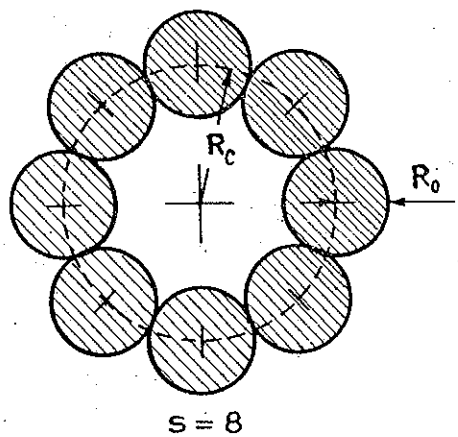

Fig. 2 — *The outer layer of a stranded conductor.*

for a given accuracy, a larger number of terms than the bundle conductor problem.

In order to preserve symmetry, the system of conductors under study will be assumed isolated in space, thereby neglecting all proximity effects due to any nearby conductors. Only the total amount of charge per unit length of the conductor under study, and not its spatial distribution, is made to depend on the geometry and potentials of nearby conductors. The errors deriving from this assumption will be acceptable as long as the distances to nearby conductors remain large compared to the transversal dimensions of the conductor system under study.

The present paper is by no means the first attempt at dealing with these problems, a rich literature is already available on the subject. However, to our knowledge, the bundle and the stranded conductor problems have always been treated separately.

Early contributions to bundle conductor theory are to be found in [1] and [2], where references are made to still earlier work. The approach taken by these authors is the classical one of considering one line charge per subconductor, and adjusting their position for a best fit with the nearly cylindrical equipotential surfaces in the immediate vicinity of the line charges.

With the advent of digital computers, a more detailed account of charge distribution becomes practical, giving rise to more sophisticated approaches, such as, the charge simulation method [3], the integral equation method [4], or the successive image method [5].

An early reference to the effects of stranding is to be found in [6]. Recent contributions to the theory of the stranded conductor may be found in [7], [8] and [9]. These authors have in common the use of a truncated series of inverse powers of the distance to the conductor axis, as a basic representation for the potential function. Fitting of the function to the boundary yields the unknown coefficients. An approximate fit is obtained in reference [7] by imposing an exact fit on a finite set of arbitrarily chosen points. In references [8] and [9] an orthogonalization procedure is carried out in a finite dimension subspace of the space of functions-over-the-boundary, the only difference being in the set of basis functions used by their respective authors.

The method used in the present paper may be regarded as a refinement of the classical method cited above in connection with references [1] and [2]. Instead of a line charge only (monopole singularity), higher order singularities (multipole singularities) are added for each conductor present. By carrying the representation to sufficiently high order any desired accuracy can be obtained. Like the classical method, it can be used with axis-parallel cylindrical boundaries in any configuration. For the bundle and stranded conductor problems, with their high degree of symmetry, it becomes particularly simple to use, requiring much less computational effort than other methods of comparable accuracy.

2 — MULTIPOLE EXPANSIONS

Consider a line charge located at the origin of the complex z-plane, with a strength of q units of charge per unit of length. The corresponding electrostatic field, for a medium of constant permittivity ε_0, may be described by the complex potential function

$$W_0(z) = A_0 \ ln \frac{1}{z} \qquad (2.1)$$

where

$$A_0 = \frac{q}{2\pi\varepsilon_0}.$$

The field described by (2.1) will be called a *monopole* field.

Now consider instead $2p$ line charges, uniformly spaced around a circle of radius ρ, having alternating positive and negative signs, and all of the same strength q (fig. 3).

The complex potential function is now given by

$$W_p(z) = \frac{q}{2\pi\varepsilon_0} \ln \frac{1+(r/z)^p}{1-(r/z)^p} \qquad (2.2)$$

where $z = Z\varepsilon^{j\theta}$ and $r = \rho\,\varepsilon^{j\alpha_p}$ denotes the position of any one of the p line charges of positive sign.

If we assume the charge distribution is now forced to concentrate at the origin by letting ρ shrink to zero, then using a power series expansion for $W_p(z)$ and retaining only the leading term, we get

$$W_p(z) = \frac{q}{\pi\varepsilon_0}\left[(r/z)^p + \ldots\right]$$

which can be taken as a sufficiently good approximation when $\rho << Z$. To obtain a finite limit for the above expression, the charge strength q is simultaneously made to grow without bound, so that in the limit we have

$$W_p(z) = A_p\left[\frac{\varepsilon^{j\alpha_p}}{z}\right]^p \qquad (2.3)$$

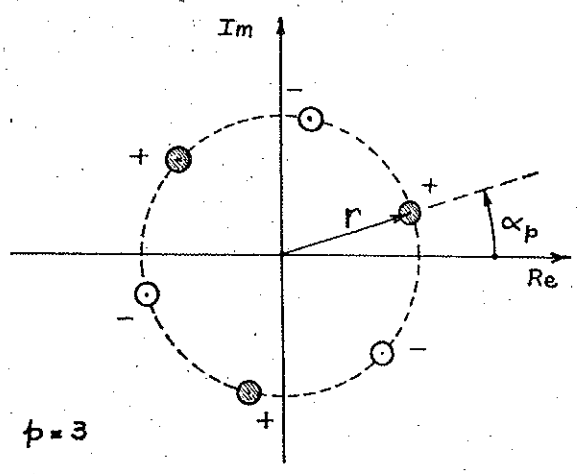

Fig. 3 — *Arrangement of line charges for a multipole of order-3.*

where A_p is a finite constant given by

$$\lim_{\substack{\rho\to 0\\ q\to\infty}} \frac{q\,\rho^p}{\pi\varepsilon_0} = A_p.$$

Expression (2.3) describes a *multipole* field of order-p. It is useful to notice the relation,

$$\frac{1}{z^p} = \frac{(-1)^p}{(p-1)!}\cdot\frac{d^p}{dz^p}\left[\ln\frac{1}{z}\right] \qquad (2.4)$$

showing that a close relationship exists, between the multipole function of order-p and the p^{th} derivative of the monopole function.

Superposition of a monopole field with multipole fields of all orders yields an expansion for the potential function having the following form

$$W(z) = A_0 \ln\frac{1}{z} + \sum_{p=1}^{\infty} A_p\left[\frac{\varepsilon^{j\alpha_p}}{z}\right]^p \qquad (2.5)$$

Taking the real part in order to obtain the actual potential function,

$$V(Z,\theta) = \mathrm{Re}\{W(z)\} =$$

$$= A_0 \ln\frac{1}{Z} + \sum_{p=1}^{\infty}\frac{A_p\cos p(\theta-\alpha_p)}{Z^p} \qquad (2.6)$$

and giving a constant value to Z, as would be the case for points on the surface of a cylinder with its axis through the origin, it is immediately seen that (2.6) represents a Fourier series development in θ for the values assumed by the potential function on that same surface. By an appropriate choice of coefficients A_p $(p = 0,1,2\ldots)$, the expansion (2.5) may be readily made to represent a potencial function assuming prescribed values over a cylindrical boundary.

3 — OFF-SET CYLINDRICAL BOUNDARIES

Instead of a cylindrical surface *coaxial* with the multipole axis, we shall now consider a cylindrical surface having an *off-set* axis (fig. 4).

For the purpose, a new complex variable x is introduced to replace z in (2.5) according to the relationship

$$x = z - z' = R\varepsilon^{j\theta} \qquad (3.1)$$

As will be easily seen, an expansion of $W(z)$ in increasing powers of variable x will lead to a Fourier series in θ, when its real part is taken, $|x|$ being held constant with a value equal to the cylinder radius. Briefly, a Taylor series expansion of $W(z)$ is required around the point $z = z'$.

For convergence reasons, the multipole axis is assumed to lie *outside* the cylinder which is equivalent to require that $|x| < |z'|$.

Writing the series in the form

$$W(z'+x) = W(z') + \sum_{m=1}^{\infty}\frac{1}{m!}\left[\frac{d^m W}{dz^m}\right]_{z=z'} x^m \qquad (3.2)$$

the coefficients, derived using (2.5), are found to be:

For the series constant term,

$$W(z') = A_0 \ln\frac{1}{z'} + \sum_{p=1}^{\infty} A_p\left[\frac{\varepsilon^{j\alpha_p}}{z'}\right]^p \qquad (3.3)$$

For the m^{th} power of x,

$$\frac{1}{m!}\left[\frac{d^m W}{dz^m}\right]_{z=z'} = \frac{(-1)^m}{m\,z'^m}\left\{A_0 + \right.$$

$$\left. + \sum_{p=1}^{\infty} A_p\, C(p,m)\left[\frac{\varepsilon^{j\alpha_p}}{z'}\right]^p\right\} \qquad (3.4)$$

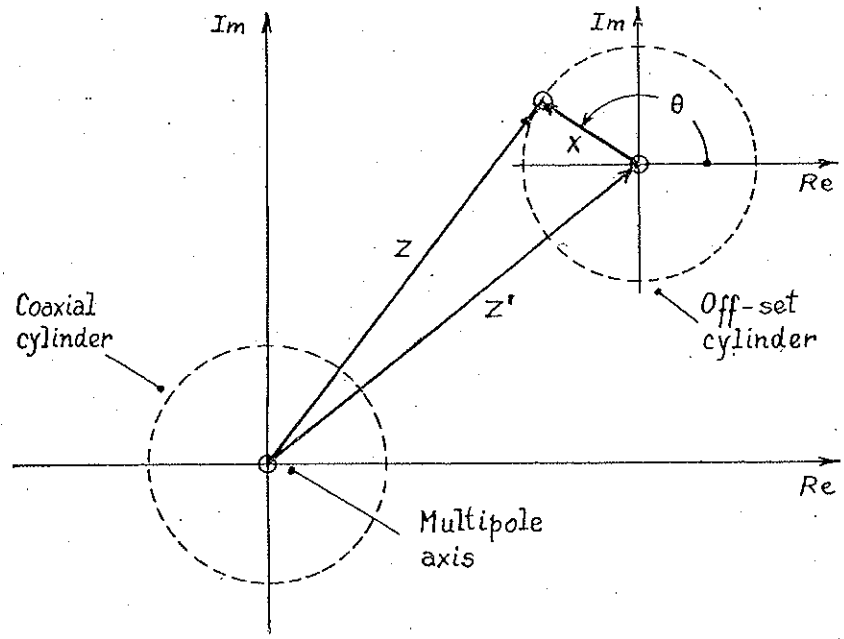

Fig. 4 — *Coaxil and off-set cylindrical surfaces.*

where

$$C(p,m) = \frac{(m+p-1)!}{(m-1)!\ \ (p-1)!} \quad . \qquad (3.5)$$

4 — THE MULTIPOLE METHOD

Assume a potential function is required satisfying prescribed boundary conditions on the surface of s cylinders, all with their axis parallel to some direction in space.

The potential function is to apply in the region of space outside the cylinders, and may be thought as the result of superposing contributions from a set of singularities, one inside each cylinder and coinciding in space with its axis. Each singularity involves in principle a monopole and multipoles of all orders.

The potential function is therefore made to depend on a set of coefficients $A_{pk}\,(p = 0, 1, 2\ldots), (k = 1, 2,\ldots s)$ the first index denoting the multipole order and the second the cylinder where it is located.

With the help of (2.5) and (3.2), expressions for the Fourier coefficients of the potential function over each boundary surface may be readily obtained in terms of the unknown A_{pk}. Expansion (2.5) is to be used for the singularities inside the cylinder under consideration and expansion (3.2) for those outside.

The boundary conditions to be imposed on the potential function now require these Fourier coefficients to assume well defined values, leading immediately to a set of linear equations in the unknown coefficients A_{pk}.

To come out with a finite numerical problem, an upper bound must be placed on index p, thereby imposing a maximum multipole order to be used in finding a numerical approximation to the exact solution.

For the important special case of conducting boundaries, all Fourier coefficients with the exception of the constant terms of each series, must be set equal to zero to insure constancy of the potential function over each conductor. The constant terms are obviously to be set equal to the potential value prescribed for the corresponding conductor.

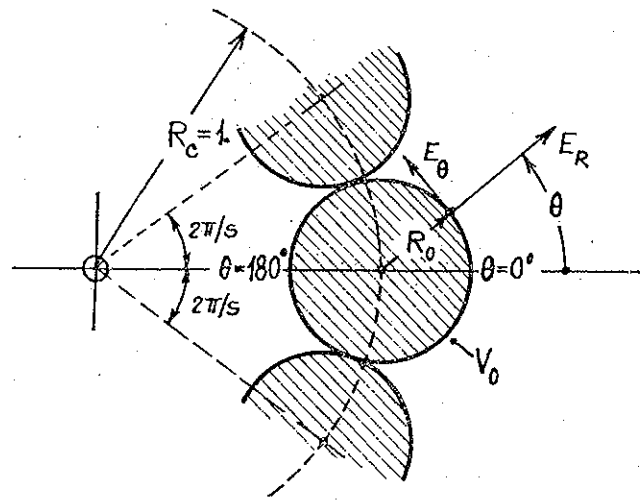

Fig. 5 — *Stranded conductor geometry.*

Experience has shown that for moderate radius to distance ratios, such as are found in connection with bundle conductors, only a few multipole terms are required for adequate accuracy. This was to be expected, since the monopole approximation already provides useful results for this type of problem.

On the other hand, the stranded conductor problem is typical for a large radius to distance ratio situation. Indeed so large as to bring the conducting surfaces into contact with each other. Here, a larger number of terms (10 to 20) may be expected to be required for high accuracy results. The computational requirements remain however, even in this extreme situation, well within practical bounds.

5 — PROBLEMS WITH N-FOLD SYMMETRY

This type of symmetry results from having the conductor axes uniformly spaced around a circle and all with the same radius. If there are s conductors and the circle radius is taken as the unit of length, the location of those axes may be denoted by

$$z_k = \varepsilon^{j\frac{2\pi}{s}k} \quad ; k = 0,1,2, \ldots s-1 \ . \quad (5.1)$$

Both the regular bundle and the stranded conductor belong in this category.

Important simplifications become possible due to symmetry. The set of unknown coeefficients A_{pk} is reduced to a set A_p independent of the conductor index k. The number of unknowns is thus reduced to the highest

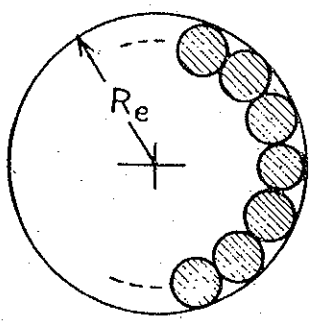

Fig. 6 — *The outer radius of a stranded conductor.*

multipole order to be considered in the approximation. Correspondingly, boundary conditions need be imposed on the surface of a single conductor only. The $k = 0$ conductor shall be used for this purpose, the off-set z' appearing in (3.2) becomes, for each conductor $k \neq 0$,

$$z' = 1 - z_k \ . \quad (5.2)$$

Symmetry also requires the spatial orientation of all multipoles to be radial. Therefore the corresponding angle α_p appearing in (3.3) and (3.4) will be given by

$$\alpha_p = \frac{2\pi}{s}k \ . \quad (5.3)$$

To add up the contributions from the $s-1$ singularities outside conductor $k = 0$, use is made of expansion (3.2) with the help of (3.3), (3.4) and (3.5). To effect the summation in k, the following results are useful,

$$\sum_{k=1}^{s-1} ln\frac{1}{1-z_k} = ln\frac{1}{s} \quad (5.4)$$

$$K_s(p,m) = (-1)^m \sum_{k=1}^{s-1} \frac{z_k^p}{(1-z_k)^{p+m}} =$$

$$= \sum_{k=1}^{s-1} \frac{\cos\left[\left(p-m\right)\left(\frac{\pi}{2} + k\frac{\pi}{s}\right)\right]}{\left(2 \text{ sen } k\frac{\pi}{s}\right)^{p+m}} \quad (5.5)$$

The total contribution from the singularities external to the $k = 0$ conductor then becomes

$$W_e(x) = A_0 \ ln\frac{1}{s} + \sum_{p=1}^{\infty} K_s(p,0)\ A_p \ +$$

$$+ \sum_{m=1}^{\infty} \frac{x^m}{m}\left[K_s(0,m)\ A_0 + \sum_{p=1}^{\infty} C(p,m)\ K_s(p,m)\ A_p\right] \quad (5.6)$$

The contribution from the singularity inside the $k = 0$ conductor is obtained by replacing z by x in (2.5) and setting $\alpha_p = 0$. The result is

$$W_i(x) = A_0 \ ln\frac{1}{x} + \sum_{m=1}^{\infty} A_m\left[\frac{1}{x}\right]^m \ . \quad (5.7)$$

Adding up both contributions, the actual potential function on the surface of conductor $k = 0$ is obtained by taking the real part of

$$W(x) = W_e(x) + W_i(x) \quad (5.8)$$

where the only complex quantity is the variable x itself.

Writing in polar coordinates,

$$x = R_0\ \varepsilon^{j\theta}$$

the real part of the logarithm terms is independent from θ, and the real part of the remaining terms is simply obtained by replacement of the x powers according to

$$Re\{x^m\} = R_0{}^m \cos m\theta \quad ; \quad Re\{x^{-m}\} = \frac{1}{R_0{}^m}\cos m\theta$$

Extracting the θ independent terms from (5.6) and (5.7) and designating by V_0 the potential value common to all conductors in the system, we have

$$V_0 = A_0 \ ln\frac{1}{sR_0} + \sum_{p=1}^{\infty} K_s(p,0)\ A_p \quad (5.9)$$

the remaining terms are

$$\sum_{m=1}^{\infty} \frac{R_0{}^m \cos m\theta}{m}\left[K_s(0,m)\ A_0 + \frac{m}{R_0{}^{2m}} A_m \ + \right.$$

$$\left. + \sum_{p=1}^{\infty} C(p,m)\ K_s(p,m)\ A_p\right] .$$

Setting N as an upper bound on p, an approximation to the expansion coefficients A_p may be obtained by solving the linear set of N equations resulting from requiring that the first N terms of the above expression be made equal to zero. This is accomplished by setting the expression in brackets equal to zero, giving

$$\frac{m}{R_0{}^{2m}} A_m + \sum_{p=1}^{N} C(p,m)\ K_s(p,m)\ A_p = -K_s(0,m)\ A_0 \quad (5.10)$$

$$m = 1, 2, 3 \ldots N$$

or, in a more compact form

$$\sum_{p=1}^{N} S_{mp} A_p = Q_m \quad ; \quad m = 1, 2, 3, \ldots N \quad (5.11)$$

The elements of the coefficient matrix being given by

$$S_{mp} = C(p,m)\ K_s(p,m) + \frac{m}{{R_0}^{2m}}\ \delta_{mp}\ ^{(1)}\ . \qquad (5.12)$$

A glance at (3.5) and (5.5) immediately shows that the first term in the above expression is symmetric for an interchange of p with m. The second term is a diagonal term and the matrix is therefore symmetric.

The independent terms on the right side of equations (5.12) coincide with the corresponding terms of (5.10) and are thus seen to be proportional to the monopole coefficient A_0,

$$Q_m = -K_s(0,m)\ \ A_0\ . \qquad (5.13)$$

The whole set of unknown coefficients A_p ($p = 1, 2, \ldots N$), is in effect proportional to A_0 because equations (5.11) are linear. This is what one would expect, given the connection of A_0 with the total charge q_T per unit of conductor length,

$$A_0 = \frac{q_T}{2\pi\ \varepsilon_0 s} \qquad (5.14)$$

this coefficient should in effect set the scale for the remaining coefficients, and through them, for the whole field.

6 — THE SURFACE FIELD INTENSITY

Accepting potential expansions truncated at the N^{th} order as sufficiently accurate approximations to the true potential function, a more compact form can be found for equations (5.6) and (5.7) by using (5.9) and (5.10) to eliminate sums over index p.

The complex potential then becomes

$$W(x) = W_e(x) + W_i(x) =$$

$$= V_0 - A_0\ ln\frac{1}{R_0} + \sum_{m=1}^{N}\frac{x^m}{m}\left[-\frac{m}{{R_0}^{2m}}\ A_m\right] +$$

$$+\ A_0\ ln\frac{1}{x} + \sum_{m=1}^{N} A_m\ \frac{1}{x^m}\ .$$

Using polar coordinates for variable x, we get for the actual potential function

$$V(R,\theta) = Re\{W(x)\} = V_0 - A_0\ ln\frac{R}{R_0} +$$

$$+\ \sum_{m=1}^{N} A_m\left[\frac{{R_0}^m}{R^m} - \frac{R^m}{{R_0}^m}\right]\frac{1}{{R_0}^m}\ \cos m\theta\ . \qquad (6.2)$$

The surface electric field intensity will now be given by

$$E_R = -\left[\frac{\partial V}{\partial R}\right]_{R=R_0}\ .$$

Differentiating (6.2), an expression for surface field intensity as a function of angle θ in terms of the expansion coefficients A_m, can be obtained

$$E_R = \frac{1}{R_0}\left[A_0 + \sum_{m=1}^{N} 2m\ \frac{1}{{R_0}^m}\ A_m \cos m\theta\right]\ . \qquad (6.3)$$

Using the above result, the average field intensity is seen to be

$$E_{av} = \frac{A_0}{R_0}\ .$$

This is the field intensity that would be observed if charge distributed itself uniformly around each subconductor surface.

The actual distribution is, however, nonuniform and as can be seen from (6.2), its maximum value occurs at $\theta = 0$.

As a direct consequence of (6.3), the ratio of maximum to average intensity is found to be

$$\frac{E_{max}}{E_{av}} = 1 + \frac{1}{A_0}\sum_{m=1}^{N}\frac{2m}{{R_0}^m}\ A_m\ . \qquad (6.4)$$

which is a fundamental result for dielectric breakdown considerations.

Another important ratio, that can be established with the help of expression (6.3) for the field intensity, is the square average to the average squared ratio,

$$\frac{(E^2)_{av}}{(E_{av})^2} = 1 + \frac{1}{{A_0}^2}\sum_{m=1}^{N} 2\left[\frac{m}{{R_0}^m}\ A_m\right]^2\ . \qquad (6.5)$$

Its importance is to be found in connection with the determination of power loss due to surface currents flowing longitudinally under conditions of intense skin effect. This will occur when, at sufficiently high frequencies, the penetration depth becomes negligible compared with the subconductor radius R_0. The current density distribution under these conditions is identical to the static surface charge distribution for the same conductor geometry. Charge density and field intensity being proportional, equation (6.5) remains valid if electric field intensity is replaced on the left side by surface current density under intense skin effect conditions.

7 — THE EQUIVALENT RADIUS CONCEPT

It is sometimes useful to relate a composite conductor to a smooth cylindrical conductor which is its equivalent from the standpoint of some important physical property. The equivalent radius of a composite conductor relative to some property is then the radius of a single cylindrical conductor, showing the same value for that property as the composite conductor.

---

(1) $\begin{cases} p = m, & \delta_{mp} = 1 \\ p \neq m, & \delta_{mp} = 0 \end{cases}$

7.1 — *THE EQUIVALENT RADIUS FOR THE POTENTIAL DIFFERENCE* R_V

At very large distances, the potential function of a composite conductor will approach that of a single line charge of strength sq, as if all charge were found concentrated on the central axis. The potential difference between a point at the surface and another point at a very large distance r_∞, will then be given by

$$\Delta V = V_0 - V_\infty = V_0 - s\,A_0\ ln\frac{1}{r_\infty}$$

according to formulation (2.1), that has been used throughout for the potential function of a line charge.

On the other hand, for a cylindrical wire of radius R_V, we would have for the same difference

$$\Delta V = s\ A_0\ ln\frac{r_\infty}{R_V}\ .$$

Equality of potential difference requires

$$R_V = \exp\,(-V_0/sA_0)$$

thereby defining an equivalent radius R_V.

Using equation (5.9) for the potential V_0 on the conductor surface, the equivalent radius may be written

$$R_V = (sR_0)^{1/s}\ \exp\left[-\frac{1}{s\,A_0}\sum_{p=1}^{N} K_s(p,0)\ A_p\right]\ .$$

The first factor $(sR_0)^{1/s}$ in the above expression is the so called «geometric mean radius» which is often used as an equivalent radius. As may be seen from the second factor, a satisfactory approximation results when the multipole terms are relatively small. The geometric mean radius is thus applicable when the radius to distance ratio is small as is usually the case for bundle conductors.

7.2 — *EQUIVALENT RADIUS FOR THE MAXIMUM SURFACE FIELD INTENSITY* R_{EM}

This may be obtained immediately in terms of the maximum to average ratio given by (6.4). In effect, we can write for the maximum field intensity

$$E_{max} = E_{av}\frac{E_{max}}{E_{av}} = \frac{A_0}{R_0}\ \frac{E_{max}}{E_{av}}\ .$$

On the other hand, for a smooth cylindrical wire of radius R_{EM} and carrying sq units of charge per unit of length, the surface field intensity would be

$$E = s\ \frac{A_0}{R_{EM}}\ .$$

Equating the above expressions, the equivalent radius is seen to be given by

$$R_{EM} = s\ R_0\ \frac{E_{av}}{E_{max}}\ .$$

7.3 — *EQUIVALENT RADIUS FOR THE INTEGRAL SQUARE FIELD INTENSITY* R_{ES}

The square field intensity integrated over the whole conductor surface may be written,

$$I = 2\pi\ R_0\ s\ (E^2)_{av} = 2\pi\ R_0\ s\ \frac{{A_0}^2}{{R_0}^2}\ \frac{(E^2)_{av}}{(E_{av})^2}\ .$$

For a smooth cylinder of radius R_{ES} carrying the same total charge per unit length sq, one would write instead

$$I = 2\pi\ R_{ES}\left[\frac{sA_0}{R_{ES}}\right]^2\ .$$

Setting the above results equal to each other, the equivalent radius R_{ES} may be expressed in terms of the ratio given in (6.5) by

$$R_{ES} = s\ R_0\ \frac{(E_{av})^2}{(E^2)_{av}}\ .$$

For computed numerical values of the above quantities relative to stranded conductors, see below in section 8.2

8 — NUMERICAL RESULTS

8.1 — *ACCURACY*

In order to test the practical feasibility of the method and simultaneously obtain results of interest for transmission line engineering regarding stranded conductor properties, a computer program was prepared to set up and solve the linear set of equations (5.11), for specified values of N, s and R_0.

It is important to notice that all quantities needed to set up equations (5.11) are directly given in closed form by formulas (3.5) and (5.5). This is in sharp contrast with the methods of references [8] and [9] which require the numerical evaluation of integrals, one per coefficient, to solve the stranded conductor problem.

Because the stranded conductor problem with its large radius to distance ratio places the highest demands on the method in what regards accuracy, it was the problem chosen to conduct the tests.

Setting $N = 20$, and choosing the monopole coefficient to be $A_0 = 1{,}0$, the results obtained for the multipole coefficients A_p are shown in Table-1 for several s values of interest. In the stranded conductor problem, the relative subconductor radius R_0 is not an independent parameter but a function of s,

$$\mathrm{R_0} = \mathrm{sen}\ (\pi/s)\ .$$

To evaluate the rate of convergence obtained, attention should be given to the coefficients in the Fourier development (2.6). These are obtained by weighing each A_p with a multiplying factor $1/Z^p$. Using $Z = R_0$, since R_0 is the shortest possible distance between a field point and a singularity, the results in Table-1

TABLE 1

	$s = 6$	$s = 12$	$s = 18$	$s = 24$	$s = 30$
	$R_0 = 0.500000$	$R_0 = 0.258819$	$R_0 = 0.173648$	$R_0 = 0.130526$	$R_0 = 0.104528$
A0	1.00000E 00	1,00000E 00	1,00000E 00	1,00000E 00	1,00000E 00
A1	3.75394E — 01	2.12911E — 01	1.46557E — 01	1.11489E — 01	8.99036E — 02
A2	3.18976E — 02	1.41742E — 02	7.23697E — 03	4.32903E — 03	2.86802E — 03
A3	— 2.31657E — 03	4.08648E — 04	2.25750E — 04	1.19527E — 04	— 6.89562E — 05
A4	— 1.06409E — 03	— 8.04520E — 05	— 1.13813E — 05	— 2.47790E — 06	— 6.84087E — 07
A5	7.80006E — 05	— 1.07157E — 05	— 1.90668E — 06	— 4.85851E — 07	— 1.62151E — 07
A6	— 6.10917E — 06	5.22201E — 07	— 3.38621E — 08	— 1.44092E — 08	— 5.12009E — 09
A7	— 6.46783E — 05	2.27884E — 07	1.37684E — 08	1.56259E — 09	2.71558E — 10
A8	— 4.41289E — 06	2.06720E — 09	1.06379E — 09	1.49268E — 10	2.83017E — 11
A9	7.87191E — 07	— 5.04616E — 09	— 8.55236E — 11	— 2.25826E — 12	1.07613E — 13
A10	3.42423E — 07	— 2.81030E — 10	— 1.58650E — 11	— 1.02572E — 12	— 1.08775E — 13
A11	— 1.04769E — 07	1.19064E — 10	2.64820E — 13	— 2.79027E — 14	— 4.45374E — 15
A12	— 2.43488E — 08	1.19717E — 11	2.06243E — 13	6.00380E — 15	3.26694E — 16
A13	1.37381E — 08	— 3.00203E — 12	5.12406E — 15	4.33040E — 16	— 3.19153E — 17
A14	1.02386E — 09	— 4.38810E — 13	— 2.53942E — 15	— 2.91453E — 17	— 5.19205E — 19
A15	— 1.68997E — 09	8.07663E — 14	— 1.65978E — 16	— 4.41921E — 18	— 1.76160E — 19
A16	1.10115E — 10	1.56631E — 14	2.99549E — 17	7.99128E — 20	— 2.87526E — 21
A17	1.88328E — 10	— 2.31952E — 15	3.51354E — 18	3.95614E — 20	8.48242E — 22
A18	— 4.15480E — 11	— 5.70094E — 16	— 3.32702E — 19	6.42133E — 22	4.17481E — 23
A19	— 1.80785E — 11	7.24285E — 17	— 6.76582E — 20	— 3.34893E — 22	— 3.58728E — 24
A20	8.58738E — 12	2.16110E — 17	3.37538E — 21	— 1.64532E — 23	— 3.52834E — 25

Table 1 — *Multipole expansion coefficients for stranded conductors.*

show that, as the order increases, the successive multipole contributions decrease in relative importance, the last terms affecting only the 5^{th} significant digit. The 20 multipole terms being considered should therefore suffice for high precision results in the stranded conductor problem. This conclusion is substantially independent from the number of strands being considered, as can be seen from the data in Table-1.

A highly sensitive test of accuracy may now be carried out by computing, using the multipole coefficients in Table-1, the potential, the radial and the tangential components of the electric field over the conducting boundary. The results for $s = 30$ are shown in Table-2. A good fit requires constant potential and zero tangential field. Furthermore, the radial field should become zero beyond the point of contact of the strands, since the cavity bounded by the conducting surfaces of the strands, looking radially inwards, should be free of any fields.

TABLE 2

$s = 30$	$R_0 = 0.104528$		$A_0 = 1.0$
θ^0	V_0	E_R	E_θ
0.0	— 2.61316	37.8545	0.0000
19.2	— 2.61316	34.7211	— 0.0014
38.4	— 2.61315	25.2085	— 0.0024
57.6	— 2.61314	10.4539	— 0.0023
76.8	— 2.61313	0.3467	— 0.0025
100.0	— 2.61316	— 0.0003	— 0.0035
120.0	— 2.61315	0.0010	— 0.0009
140.0	— 2.61315	0.0007	0.0003
160.0	— 2.61315	— 0.0001	0.0005
180.0	— 2.61315	— 0.0004	0.0000

Table 2 — *Surface potential and field components. See fig. 5.*

As far as the electric field is concerned, and relative to its maximum value, the results in Table-2 meet the above requirements to better than 1 part in 10 thousand.

The significance of potential function errors may be obtained by dividing them by the radial field intensity and interpreting the result as a shift between the computed equipotential surface and the actual conductor surface. These shifts are negligible over the whole surface down to the points of contact $\theta = 96°$.

Finally in Table-3 results obtained by the multipole method are compared to results found in reference [8] for the same problem. To adapt to the mode of presentation used in reference [8], it is only necessary to multiply the results found for E_R, such as those in Table-2, by an appropriate constant (2). The results agree to the 5^{th} decimal place, except near the point of contact where, as the authors of reference [8] point out, their method is expected to fail.

From the evidence presented above the conclusion can be reached that the multipole method may be used with confidence to solve the stranded conductor problem, and with greater reason the bundle conductor problem too, comparing favourably with other possible methods while requiring a very modest computational effort (3).

(2) *See Apendix 1.*

(3) *All numerical results in this paper have been obtained using a desk type programmable calculator Tektronix model Tek-31 with 12 decimal digit mantissa.*

TABLE 3

$s = 30$	E_R Vcm^{-1}/V	
θ^0	*This paper*	*Ref.* [8]
0.0	0.100701	0.100706
9.6	0.098635	0.098630
10.6	0.092365	0.092370
28.8	0.081849	0.081846
38.4	0.067060	0.067060
48.0	0.048449	0.048452
57.6	0.027810	0.027803
67.2	0.009739	0.009750
76.8	0.000922	0.000911
86.4	0.000002	0.000007
96.0	0.000000	0.000230

Table 3 — *Comparison of field intensity distributions. See Apendix I for details of conversion to the mode of presentation used in reference* [8].

TABLE 4

s	R_V	R_{EM}	R_{ES}
2	0.785398	0.636614	0.750000
4	0.906481	0.700248	0.854211
8	0.954243	0.713573	0.890572
12	0.969515	0.715829	0.901312
18	0.979648	0.716986	0.908166
24	0.984717	0.717386	0.911508
30	0.987762	0.717547	0.913488
∞	1.000000	0.717759	0.921227

Table 4 — *Equivalent radii of stranded conductors, the outer radius being taken as unity. See fig. 7.*

8.2 — *STRANDED CONDUCTOR EQUIVALENT RADII*

Using the expressions derived in section 7., the equivalent radii may be easily computed from the multipole coefficients A_p found for each strand number s. The results appear in Table-4 and may be seen plotted in fig. 7. The attention of the reader is called to the fact that the *outer* radius R_e of the stranded conductor has been taken as unity.

To facilitate further use of these results in digital computer programs, interpolation formulas of sufficient accuracy were developed which are usable for $s \geqslant 2$, with the absolute errors as indicated below.

1) For the potential difference:

$$R_V = \left[a - \frac{s}{b_0 s^2 + b_1 s + b_2} \right] R_e$$

a = 1.0 Errors:
b_0 = 2.7104877 $\varepsilon_{max} = -1.9\text{E}-4$ for $s = 3$
b_1 = 0.4811760
b_2 = −2.4847182 $\varepsilon < 2.6\text{E}-6$ for $s \geqslant 8$

2) For the maximum field intensity:

$$R_{EM} = \left[a - \frac{1}{b_0 s^3 + b_1 s^2 + b_2 s + b_3} \right] R_e$$

a = 0.717760 Errors:
b_0 = 7.94105E − 2 $\varepsilon_{max} = 3.2\text{E}-4$ for $s = 3$
b_1 = 2.72957 $\varepsilon < 6.4\text{E}-5$ for $s \geqslant 18$
b_2 = 3.79121
b_3 = −6.81212

3) For the integral square field intensity:

$$R_{ES} = \left[a - \frac{s}{b_0 s^2 + b_1 s + b_2} \right] R_e$$

a = 0.92122679 Errors:
b_0 = 4.3856939
b_1 = −2.3071869 $\varepsilon_{max} = 4.0\text{E}-5$ for $s = 3$
b_2 = −1.2479854 $\varepsilon < 1.2\text{E}-6$ for $s \geqslant 6$

The reader may have noticed that for each radius, a precise limiting value has been given above, corresponding to a conductor with an infinite number of strands.

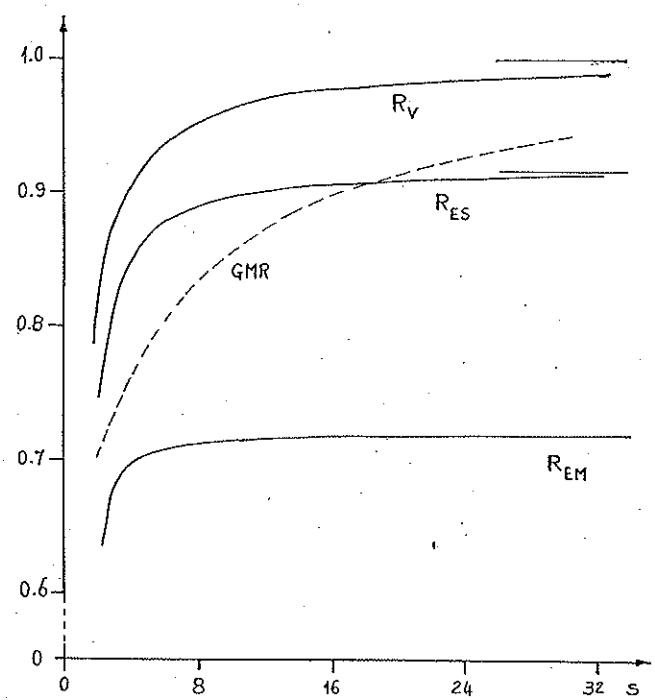

Fig. 7 — *Equivalent radii of stranded conductors, the outer radius being taken as unity. See fig. 6. GMR is the «geometric mean radius».*

These limiting values were obtained by solving the electric field problem of a *plane* grating of cylindrical wires thick enough to touch one another, as the strands do in a stranded conductor. The plane grating provides the proper description of the local situation on a stranded conductor surface when the distance between consecutive strands becomes, in the limit, much smaller than the conductor radius.

The plane grating problem has been solved using the multipole method.

8.3 — *ELECTRIC FIELD INTENSITY DISTRIBUTION AROUND A STRAND*

Making use of equation (6.3), the field intensity may be readily obtained as a function of θ, once the A_p are known.

A family of curves obtained by varying the strand number s are plotted in fig. 8. Unity on the ordinate axis represents the field strength at the surface of a smooth cylinder having a radius equal to the outer radius R_e of the stranded conductor and bearing the same charge per unit length.

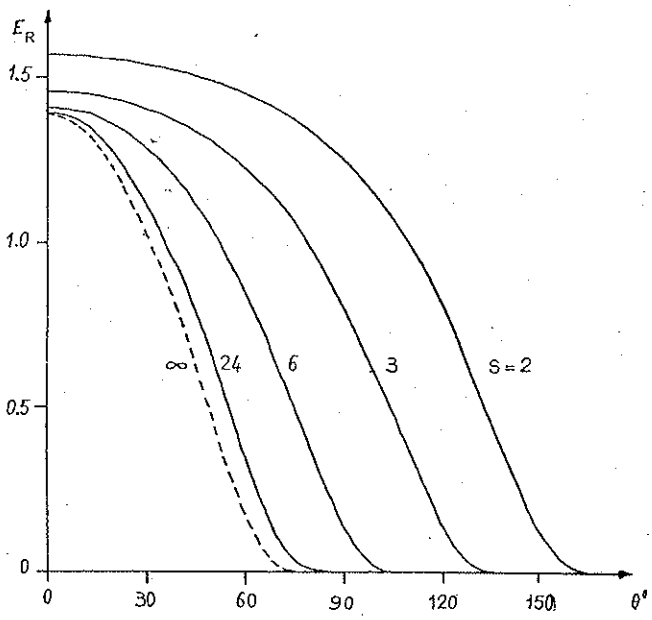

Fig. 8 — *Field intensity distribution. Unit intensity represents field on a smooth cylinder of radius R_e, see fig. 6, bearing the same charge.*

The maximum field intensity occurs at the tip of the strand (θ = 0) and its value varies little with the strand number s. This fact was already patent in the flatness of the R_{EM} curve that can be observed in fig. 7. Several authors, [6] and [7], have pointed out that stranding entails an increase of about 40 % in maximum field intensity for large s values. The exact limiting value is 39.3 %.

9 — CONCLUSIONS

Potential problems involving cylindrical boundaries have been found capable of an efficient solution to a high degree of accuracy through the use of the multipole method.

The method was successfully applied to the stranded conductor problem which, being an extreme case with a large conductor radius to distance ratio, may be taken as a severe test on its range of applications.

The numerical results that have been obtained for the stranded conductor configuration confirm and under certain particular aspects improve published results obtained by different authors, using other methods.

Properties of stranded conductors, important for power transmission line engineering, have been expressed using the equivalent radius concept and the latter have been computed as a function of strand number. Interpolation formulas, depending on a few parameters only, were developed to facilitate use of these results in digital computer programs.

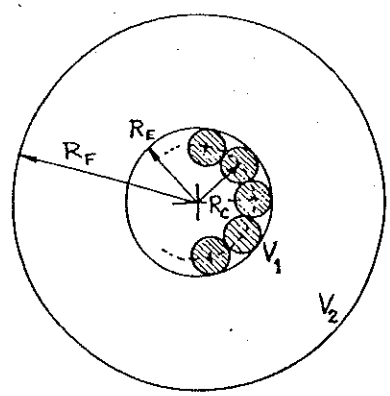

Fig. 9 — *Coaxial arrangement used in reference* [8].

APENDIX 1

In reference [8], numerical results are computed on the basis of a coaxial arrangement having the stranded conductor under study as the center conductor (fig. 9). The corresponding monopole coefficient will then be given by

$$A_0 = q/2\pi\varepsilon_0 = C(V_1 - V_2)/2\pi\varepsilon_0 s$$

where the capacitance per unit length C is to be found using

$$C = 2\pi\varepsilon_0/ln\,(R_F/R_E R_V) \quad .$$

The radius R_0 of the circle passing through the strand cross section centers is given in terms of R_e by

$$R_C = R_E/[1 + \text{sen}\,(\pi/s)] \quad .$$

To enable a comparison of values such as those given in Table-2 of this paper that were obtained for $A_0 = 1.0$, $R_c = 1.0$ to the corresponding values in reference [8], a multiplying constant A_0/R_c is to be applied to the results of Table-2, where A_0 and R_c result from entering the values used in reference [8] in the above expressions. These are

$$R_F/R_E = 1\,000 \qquad R_E = 2 \text{ cm}$$

$$V_1 - V_2 = 1\ V \qquad s = 30$$

from Table-4 we further take for $s = 30$, $R_V = 0.987762$, then the appropriate multiplier is

$$A_0/R_C = 2.66021\text{E} - 3 \quad Vcm^{-1}$$

10 — REFERENCES

[1] M. TEMOSHOK, «Relative Surface Voltage Gradients of Grouped Conductors», AIEE Trans. pt. II, Vol. 67, pp. 1583-1591, 1948.

[2] A. S. TIMASCHEFF, «Field Patterns of Bundle Conductors and Their Electrostatic Properties» AIEE Trans. pt. III, Vol. 80, pp. 590-597, October 1961.

[3] M. S. ABOU-SEADA, E. NASSER, «Digital Computer Calculation of the Potential and its Gradient of Twin Cylindrical Conductor», IEE Trans. Power Apparatus and Systems, Vol. 88, pp. 1802-1814, December 1969.

[4] P. Y. Foo, S. Y. King, «Bundle-conductor electric field by integral equation method», Proc. IEE, Vol. 123, pp. 702-706, July 1976.

[5] M. P. SARMA, W. JANISCHEWSKIJ, «Electrostatic Field of a System of Paralell Cylindrical Conductors», IEE Trans. Power Apparatus and Systems, Vol. 88, pp. 1069-1079, July 1969.

[6] W. A. LEWIS, (Discussion of paper in Ref. [1] above), AIEE Trans. pt. II, Vol. 67, pp. 1589-1590, 1948.

[7] J. G. ANDREWS, A. J. SCHRAPNEL, «Electric Field distribution around an isolated stranded conductor», Proc. IEE, Vol. 119, pp. 1162-1166, August 1972.

[8] H. PAREKH, M. S. SELIMA, E. NASSER, «Computation of electrical field and potential around stranded conductor by analytical method and comparison with charge simulation method», Proc. IEE, Vol. 122, pp. 547-550, May 1975.

[9] W. SCHNIDER, H. BAGGENSTOS, «Computation of Electrical Field around Stranded Conductors Using Orthogonal Functions», Archiv für Elektrot., Vol. 60, pp. 41-45, 1978.